Fish and Shellfish Immunology 86 (2019) 934–941

Contents lists available at ScienceDirect

Fish and Shellfish Immunology

journal homepage: www.elsevier.com/locate/fsi

Full length article

Shell repair and the potential microbial causal in a shell disease of the pearl oyster *Pinctada fucata*

Jingliang Huang[a], Liping Xie[a], Rongqing Zhang[a,b,*]

[a] MOE Key Laboratory of Protein Sciences, School of Life Sciences, Tsinghua University, Beijing, 100084, China
[b] Department of Biotechnology and Biomedicine, Yangtze Delta Region Institute of Tsinghua University, Jiaxing, 314000, China

ARTICLE INFO

Keywords:
Pearl oyster
Shell repair
Disease
Hemocyte

ABSTRACT

The pearl oyster *Pinctada fucata* is famous for producing luxurious pearls. As filter feeders, they are confronted with various infectious microorganisms. Despite a long history of aquaculture, diseases in *P. fucata* are not well studied, which limits the development of the pearl industry. We report here a shell disease in *P. fucata* and a study of the shell repair processes. Scanning electron microscopy (SEM) revealed that the nacreous layer gradually recovered from disordered $CaCO_3$ deposition, accompanied by a polymorphic transition from a calcite-aragonite mixture to an aragonite-dominant composition, as revealed by X-ray diffraction analysis. SEM also showed that numerous microbes were embedded in the abnormal shell layers. Similar indications were induced by a high concentration of microbes injected into the extrapallial space, suggesting the potential pathogenic effect of uncontrolled microbes. Furthermore, hemocytes were found to participate in pathogens resistance and might promote shell repair. These results further our understanding of pathogen-host interactions in pearl oysters and have implications for biotic control in pearl aquaculture.

1. Introduction

Pinctada fucata is one of the most important bivalve genera that produce cultured pearls. The oyster shell resembles the pearl in microstructure, so during the past decades, it was attractive for intensive studies to elucidate the mechanism underlying shell formation [1–3]. However, our knowledge of pathology and immunity in *P. fucata* is relatively sparse, even though perliculture has been developed for over one hundred years since the first cultured pearl was produced [4]. Our lack of knowledge led to large economic loses during shellfish disease outbreak. For example, mass mortality was associated with a viral disease in *P. fucata* in both 1996 and 1997, resulting in an annual mortality of over 400 million individuals [5]. Intensive studies are required to elucidate the epidemiology of serious diseases, which cause dramatic mortality and to provide efficient protective solutions.

The shell of *P. fucata* is composed of two calcified layers, an inner nacreous layer and an outer prismatic layer. Usually, the prismatic layer is covered with the thin organic membrane known as periostracum. In pearl oysters, the mantle tissue is responsible for shell formation, the outer mantle edge for the periostracum and prismatic layer, and the inner pallial zone for the nacreous layer [6]. An organic matrix secreted by the mantle tissue self-assembles into a framework and directs $CaCO_3$ precipitation in the extrapallial space (EPS). In addition, hemocytes are supposed to participate in shell formation by providing organic matrix and crystal materials [7–9], especially in particular situations such as shell damage and shell disease. Precisely cellular control of the microenvironment in the EPS is required and any disturbance of homeostasis would affect shell formation [10,11].

Abnormal shell precipitation has been reported in clam and oysters [12–14]. Gram-negative bacteria of the genus *Vibrio* have been frequently found to be the infectious agent in many reported shell diseases [13,15], and the pathogenesis of *Vibrio* showing the disease signs was experimentally reproduced in larval oysters [16]. The well-studied Juvenile Oyster Disease (JOD), also known as *Roseovarius* Oyster Disease (ROD), has been blamed on a *α-Proteobacteria, Roseovarius crassostreae,* which causes abnormal conchiolin deposition in the cultured oyster *Crassostrea virginica* [17]. Additionally, fungi and parasites were responsible for shell disease in the oysters *Osrea edulis*, *Crassostrea angulata*, and *Crassostrea virginica* [18,19] and in the clams *Ruditapes decussates* and *Mercenaria mercenaria* [20,21]. The studies mentioned above mainly focused on the histopathological modifications of the tissues and shell, yet provided very little evidence of the crystal structure of the shell in general. Furthermore, shell diseases in the genus *Pinctada* have not been well studied.

Our group has worked for years on shell formation in *P. fucata* [3,22]. Shell diseases have been frequently observed. Particularly, some

* Corresponding author. MOE Key Laboratory of Protein Sciences, School of Life Sciences, Tsinghua University, Beijing, 100084, China.
E-mail address: rqzhang@mail.tsinghua.edu.cn (R. Zhang).

https://doi.org/10.1016/j.fsi.2018.12.032
Received 23 July 2018; Received in revised form 13 November 2018; Accepted 18 December 2018
Available online 19 December 2018
1050-4648/

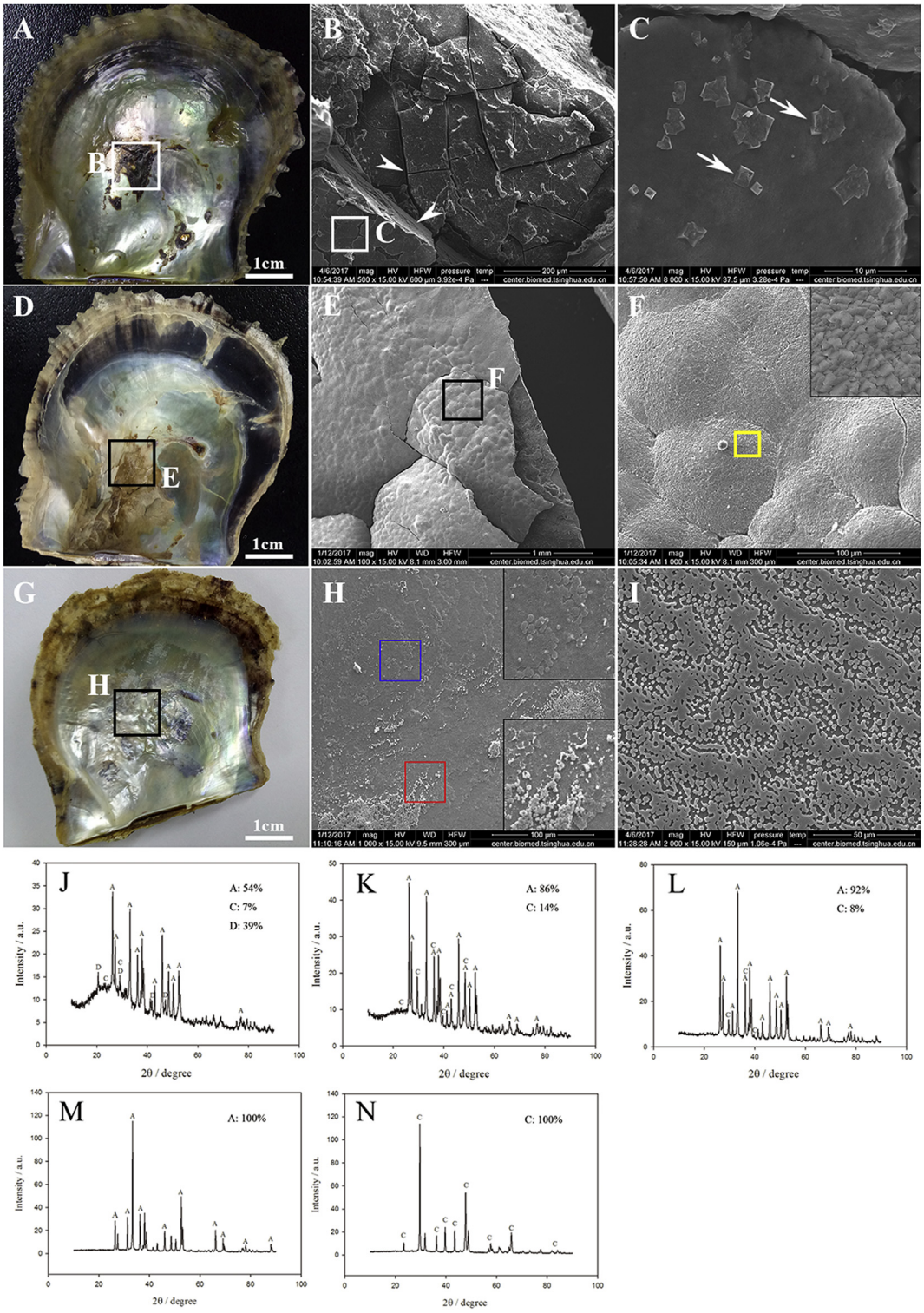

Fig. 1. The microstructure and crystal polymorphs of the diseased shell surface of the nacreous layer during the shell repair process. A-C, shell repair stage I.B and C are magnifications of the white frames in A and B, respectively. White arrowheads in B indicate the straight progression along the crack in the deposits. White arrows in C indicate the cubic crystals on the surface of the deposits. D-F, shell repair stage II. E and F are magnifications of the black frames in D and E, respectively. Magnification of the yellow frame in F is shown in the upper right corner. G-H, shell repair stage III. H is the magnification of the black frame in G. Insets at the upper and bottom right corners in H represent the magnifications of the blue and red frames, respectively. I, inner surface of the normal nacre layer. B-C, E-F, H-I are SEM images. J-N, an XRD analysis of the inner surface of different shell samples. J-L, samples from shell repair stages I, II, and III, respectively. M and N, normal shell layers of nacre and prism, showing the standard XRD graphs of aragonite and calcite. a, aragonite; c, calcite; d, monohydrate calcite. (For interpretation of the references to color in this figure legend, the reader is referred to the Web version of this article.)

individuals bear abnormal brown deposits on the inner 91 layer of the nacre. The appearance and texture of the deposits are very different from the shiny nacre. 92 And the heterogeneous distribution and abnormal morphology after recovery indicate their 93 pathological origin rather than environmental perturbation. In the current study, we reported an investigation of the abnormal deposits in the nacreous shell layers of *P. fucata*. The shell repair process and the potential etiological factors were studied.

2. Materials and methods

2.1. Samples collection

Pearl oysters were purchased from Guangdong Ocean University (Zhanjiang, China), and kept in 600 L tanks with artificial sea water (ASW). Live adult individuals of *P. fucata* were sacrificed and the somatic body mass was removed with a dissecting knife. Shell samples of dead specimens were collected directly from the tank. All of the shells were cleaned with tap water and air dried at room temperature. Shell samples were divided into normal and diseased groups by examining the inner surface of the shell. The abnormal shells exhibited some shade color and matte deposits while the normal ones are smooth and shiny.

2.2. SEM observation and analysis of the crystal forms

Shell samples from six individuals were cut into small pieces and coated with gold for 60 s. Then the shell surface was examined using a scanning electron microscope (FEI Quanta 200) with an accelerating voltage of 30 kV in a high vacuum mode. To determine the crystal forms, the abnormal deposits on the inner surface of the nacre were scraped and carefully collected with a dissecting knife, then X-ray diffraction (XRD, D8 ADVANCE, Bruker, Germany) or Laser Raman Spectroscopy (Evolution, HORIBA, France) was performed. The scanning angle of the XRD was 0–90°. The wavenumber of Raman spectrum ranged from 100 to 1200 cm^{-1}. For XRD analysis, deposit samples were collected from 10 to 15 oysters in each group, and for Raman spectrum, six samples were examined in each group.

2.3. Decalcification of the shell and hematoxylin-eosin staining

The oyster shells were cut into pieces with a glass cutter and scissors. Decalcification was accomplished by soaking the shell pieces in 400 ml EDTA (0.25 M, pH 8.0) for 72 h at room temperature. The decalcified shells were fixed in 4% paraformaldehyde, then the shells were subjected to dehydration in an ethanol gradient, and subsequently paraffin-embedded. The paraffin blocks were sectioned (5 μm) and stained with hematoxylin-eosin (HE) using a standard histological procedure. Stained sections were examined using a light microscope (TieU, Nikon, Tokyo, Japan).

2.4. Shell disease induced by injected microbes

The gram-negative bacterium *Escherichia coli* (DH 5α, TaKaRa, Japan) and the beer yeast *Saccharomyces cerevisiae* carrying a YFP reporter gene were cultured to the logarithmic growth phase in appropriate culture media. The pellets were collected by centrifugation and washed with sterile sea water. Then the pellets were re-suspended in sterile sea water and adjusted to specific concentrations. In this study, low dosage of microbe injection was defined as 10^7 CFU/ml for *S. cerevisiae* and 10^8 CFU/ml for *E. coli*, and high dosage of microbe injection was defined as 10^9 CFU/ml for *S. cerevisiae* and 10^{10} CFU/ml for *E. coli*, respectively. To eliminate the possibility that the induced shell disease might be ascribed to the physical irritation of the injected microbe pellets, commercial $CaCO_3$ (calcite, MACKLIN, analytically pure) suspension containing 10 mg $CaCO_3$ in 1 ml sterile sea water, with the concentration equal to the microbe suspensions, was used as a control. Before injection, the pearl oysters were anesthetized with 0.2% phenoxy propyl alcohol, and then 100 μl microbes, $CaCO_3$ suspension or sterile sea water were injected into the extrapallial space of the Left valve. 30 individuals were used in each treatment. The oysters were returned to the tank and collected for examination after one month.

To analyze hemocytes phagocytosis, yeast was injected into the EPS as described above. Six oysters were collected after 24 h. The extrapallial fluid was extracted with a 1-ml syringe and examined using a fluorescence microscope (TieU, Nikon, Tokyo, Japan). Because the YFP channel is absent in this type of microscopy and the excitation wavelength of YFP is 500 nm (bandwidth 20 nm), we used the green channel (488 nm) to photograph the YFP-yeast.

3. Results and discussion

3.1. Shell repair processes in the shell disease

Abnormal shell deposits were found both in oysters that died naturally and live individuals. These samples were classified into three groups according to the extent of the shell repair: stage I (Fig. 1A), stage II (Fig. 1D) and stage III (Fig. 1G). For the sake of simplicity, the positions where the abnormal deposits located in the pallial nacreous layer or central nacreous layer were excluded for classification purposes.

Generally, stage I shells contained dark brown deposits, which were soft and easily curled up during the air-drying process. When observed with SEM, the microstructure was rather disordered. Fig. 1B shows that some chaps on the surface of the deposit resemble the cracks in sun-baked riverbeds. Interestingly, numerous cuboidal crystals of several microns in length were deposited on the flattened surface and integrated into the previous-formed amorphous layer (Fig. 1C). These crystals were similar to cubic calcite formed in vitro [23] and supposed to be precursors of the regenerated shell. Consistently, cubic calcite presumably secreted by hemocytes were found on the newly regenerated shell in *Crassostrea virginica* and quickly remodeled into shell layers [24]. The XRD results showed that the deposited material contained aragonite, calcite and monohydrate calcite (Fig. 1J), with respective content of 54%, 7% and 39%. The basal line was relatively high compared to the pure nacreous and prismatic layer (Fig. 1M and N), suggesting a low degree of crystallization [25,26].

Shell repair stage II was evidenced by a gray, brittle, solid lamella covering the affected area. Complex morphologies were found during shell repair stage II. New prism sheets were formed right above the pallial nacre layer (see in section 2.2), while mixed and irregular deposits were present inside the central fossa. As shown in Fig. 1E, the regenerated shell layers were deposited on the previous nacreous layer but clearly detached from the latter indicating that they were formed de novo, different from the continuing growth of nacre sheets. The swelled layer consisted of randomly stacked flakes measuring several microns in diameter (Fig. 1F). However, these flakes were different from the tablets in the normal nacre; the latter was regularly shaped and stacked in order. In stage II, the crystal composition became dominant over the soft organic materials, and the calcite content decreased to 14%, replaced by increasing aragonite (Fig. 1K).

The shell was completely repaired in stage III. Although the repaired area was easily discerned due to its uneven surface, the shiny layer resembled normal nacre. This was confirmed by an SEM observation showing that although some irregular deposits existed, most of the area was covered by ordered nacreous sheets (Fig. 1H), similar to the normal nacreous layer (Fig. 1I). The calcite content further decreased to 8%, and the basal line went down to near zero (Fig. 1L), suggesting a recovery of crystal composition from a heterogeneous mixture.

The shell repair process in *P. fucata* was consistent with previous studies on the progressive shell repair in several molluscs in shell disease or artificial shell damage [27–29]. When brown ring disease was reproduced in Manila clams, small pustules and the periostracum were

first laid down on the shell surface, following the expansion of bacterial invasion [29]. Similarly, we found that the brown deposit in stage I in *P. fucata* was highly organic, although its chemical composition was not clear. Subsequently, polymorphs of the abnormal deposits gradually shifted from a calcite/aragonite mixture to pure aragonite, which was consistent with a previous study in *Pomacea paludosa* [30]. Calcite precipitation in nacreous layers found the present study is a very interesting phenomenon. Generally, nacreous layers in pearl oysters exclusively consist of aragonite, while prismatic layers in marine bivalves contain calcite. Considering the high Mg: Ca ratio (~5.2) and high concentration of SO_4^{2-} in the ambient sea water, calcite precipitation is severely hindered [31]. Still, *P. fucata* produces calcitic layers covering the inner nacreous layers and the depositions of prism and nacre were controlled by different secretory repertoires [3,32]. Obviously, the regular nacre precipitation in the EPS might be disrupted by the shell disease, and the infectious agents induced a genetic switch in the mantle tissue such that calcite deposition was promoted. After the formation of calcite-matrix primer, deposition of ordered aragonitic tablets gradually recovered. Similar results were also found during flat pearl formation in abalone [33] and pearl oyster [34]. More studies are needed to unravel the interfacial recognition by the mantle tissues.

3.2. Re-initiation of mineralization sequence in the natural diseased oysters

A special type of shell repair frequently occurs in the pallial zone of the nacreous layer (Fig. 2A). A thin transparent shell layer was found to cover the affected site, whose edge was parallel to the former prism layers, and it was completely separated from the former shell layers, indicating its de novo formation. Microscopy clearly revealed the polygonal structure of the regenerated prismatic layer (RPL, Fig. 2B), and the RPL grew on the former layers of nacre (Fig. 2C), in a reversal of the normal order of prism-nacre growth sequence. Raman analysis confirmed that calcite predominated in the RPL (Fig. 2D–F).

In normal shell formation, the prismatic layer grows on the periostracum, followed by the precipitation of the nacreous layer. In an emergency, for example in artificial shell damage, the prism-secreting mantle edge would retract to the pallial nacreous layer (personal observation). A severe shell disease may have the same effect. The retracted mantle edge secretes a prismatic layer over the diseased site in the pallial nacreous layer. In this manner, the potential causal agents become segregated, and the shell disease is controlled.

3.3. Shell disease caused by the uncontrolled growth of microbes in the EPS

To investigate the pathology of the shell disease, we examined the shells in detail by removing the abnormal deposits. SEM images (Fig. 3A and B) showed that, beneath the abnormal deposits, there were numerous bacteria-like rods with several hundred nanometers in diameter and 1–3 μm in length. Among them, some hemocytes-like granules were found, with the size similar to the small hyalinocytes in *P. fucata* [35].

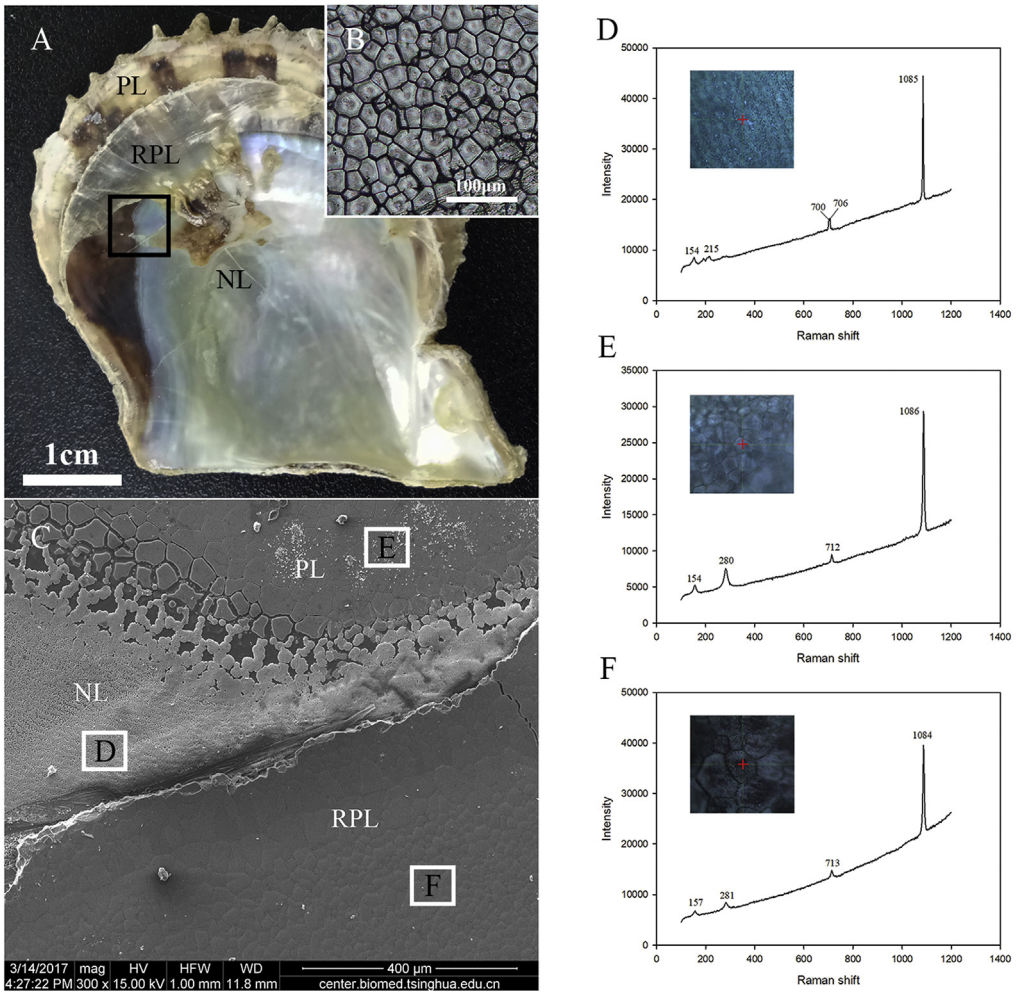

Fig. 2. Shell regeneration in the pallial nacreous layer. A, an overall view of the regenerated shell, showing the regenerated prismatic layer above the previous prismatic layer. B, microphotograph of the RPL area (phase contrast mode). C, SEM of the black framed area in A. D-F, Raman analysis of the crystal composition in the normal nacreous layer (D), normal prismatic layer (E) and regenerated prismatic layer (F). PL, prismatic layer; RPL, regenerated prismatic layer; NL, nacreous layer.

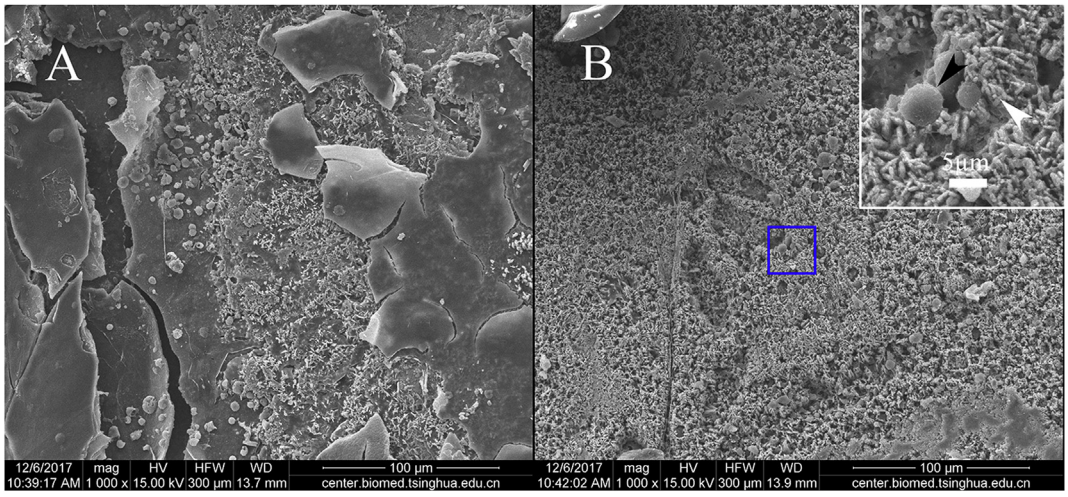

Fig. 3. Scanning electronic microscopy of the nacreous layers from the diseased oysters with abnormal shell deposits partially (A) or totally removed (B). Insert in b is the magnification of the blue frame, showing numerous rod-shape microbes (white arrow head) and hemocyte-like cells (black arrow head). (For interpretation of the references to color in this figure legend, the reader is referred to the Web version of this article.)

In a previous study we had showed that the EPS between the mantle and the shell surface contained certain amount of microbes [36]. Therefore, we speculated that uncontrolled growth of these microbes might affect the mineralization process and lead to shell disease.

To test this hypothesis, we injected concentrated microbes into the EPS to induce shell disease. Because the natural pathogenic microbes have not been identified, we used the gram-negative bacterium *E. coli* and the beer yeast *S. cerevisiae* to infect the oysters. As a result, similar signs of serious shell disease were reproduced by high dosage of microbe injections (Fig. 4G and K, Table 1). Both bacterium and yeast showed high pathogenicity, leading to 100% (27 out of 27 individuals) and 95.8% (23 out of 24 individuals) of diseased oysters, respectively. The appearance of the brown deposits resembled those in shell repair stage I of the naturally diseased oysters, as shown by the SEM examination (Fig. 4H and L). The microstructure of the inner surface of

Table 1
Artificially-induced shell disease injected with various materials.

Injected materials	Oysters with sign of shell disease (diseased/total)	
	Left valve	Right valve
Sterile sea water	3/24[a]	0/24
CaCO3 (calcite)	5/27	0/27
E. coli (low dosage)	7/28	0/28
E. coli (high dosage)	27/27	1/27
S. cerevisiae (low dosage)	6/26	0/26
S. cerevisiae (high dosage)	23/24	2/24

[a] The total number represents the survived oysters after one month.

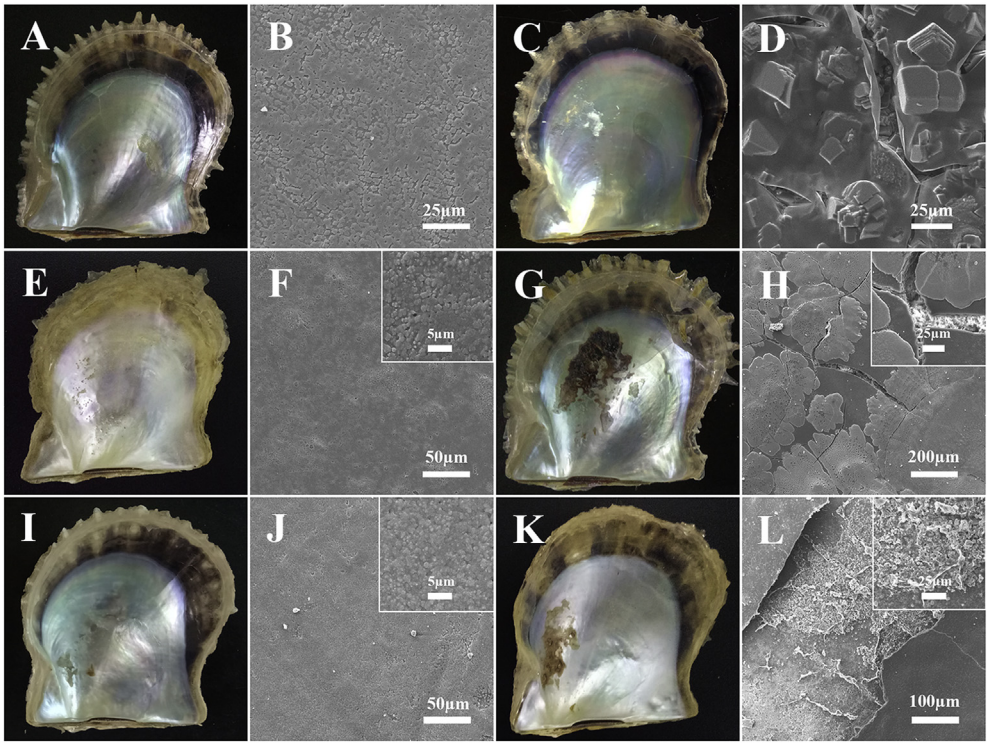

Fig. 4. Artificially-induced shell disease in *P. fucata*. A, C, E, G, I and K are digital pictures; B, D, F, H, J and L are SEM images. A and B, shell samples from oysters injected with sterile sea water. C and D, shell samples from oysters injected with calcite particles. E-H, shell samples from oysters injected with low dosage (E and F) and high dosage (G and H) of bacteria *Escherichia coli*. Insets in F and H are magnification of F and H, respectively. I-L, shell samples from oysters injected with low dosage (I and J) and high dosage (K and L) of yeast *Saccharoyces cerevisiae*. Insets in J and L are magnification of J and L, respectively.

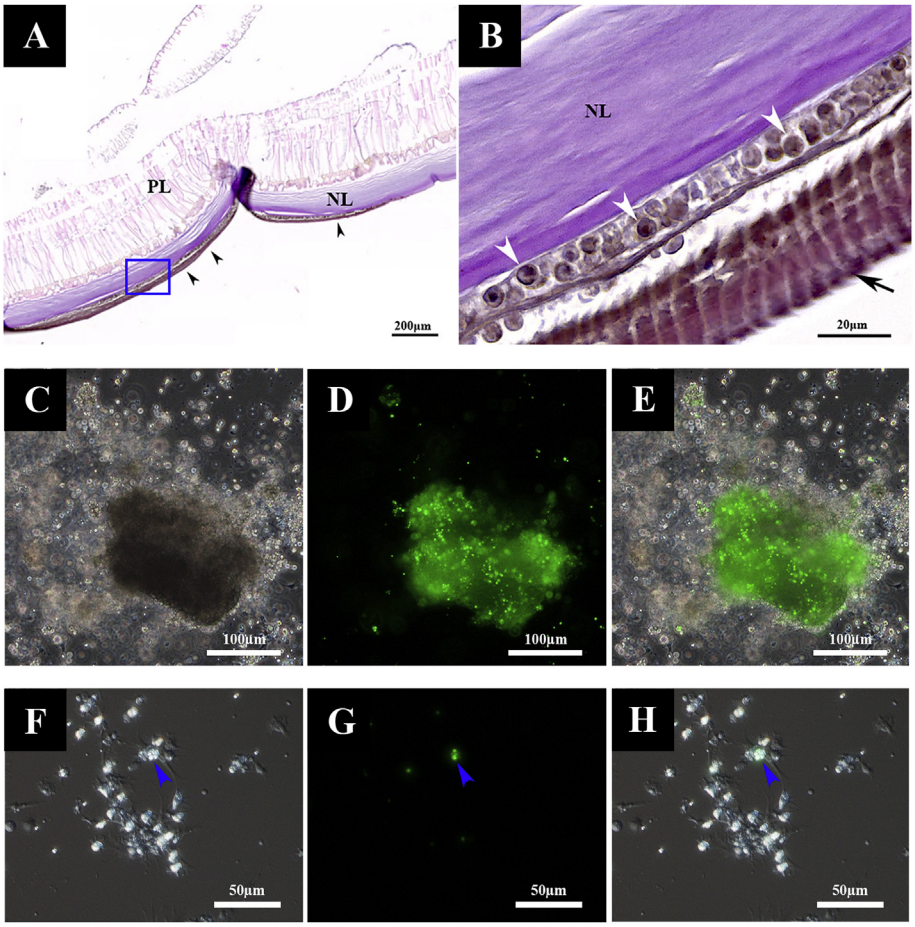

Fig. 5. Participation of hemocytes in shell repair. A, hematoxylin-eosin staining of the decalcified shell containing the infection site in a naturally-diseased oyster, lateral view. Black arrow heads indicate the abnormal deposits on the nacreous layers. B, magnification of the blue box in A. White arrow heads indicate the granulocyte-like hemocytes buried in the shell layers. Black arrow indicates the abnormal deposits. C-H, Light microscopy images showing the agglutination (C–E) and phagocytosis (F–H) of yeast by hemocytes in the EPS. C and F, bright field; D and G, green channel, showing the yeast; E, merge of C and D; H, merge of F and G. The blue arrow heads indicate the phagocytosis of the injected yeast by hemocytes. PL, prismatic layer; NL, nacreous layer.

the nacreous layers was dramatically changed and no longer precipitated in order. In contrast, most of the oysters injected with sterile sea water or low dosage of microbe showed no symptoms (Fig. 4A, E and 4I, Table 1), although the nacre tablets formation was affected by the injected microbes of low dosage (Fig. 4F and J) compared to the control group (Fig. 4B). We selectively conducted the injection in the EPS of the Left valve, and examined both valves of the shells. The results (Table 1) clearly show that the signs of disease were exactly caused by the injection operation rather than affected by the anaesthetization or by other interferences. Therefore, large amount of microbes in the EPS could cause serious shell disease in *P. fucata*. Moreover, such symptom could not be induced by injected calcite powders (Fig. 4C), eliminating the possibility that the induced shell disease might due to physical irritation of the microbe particles. Nevertheless, the calcite particles disrupted the nacreous layer deposition and were covered by an organic membrane (Fig. 4D). This membrane might contribute to segregate the particles since the aragonitic tablets could not grow directly on the calcite.

Shell formation occurs in the EPS, where microbes and protozoa occasionally penetrate. Furthermore, the extrapallial fluid (EPF) contains proteins, lipids and polysaccharides, which is an excellent medium for microbial growth. And a certain amount of microbes was contained in the EPF of *P. fucata* [36], which might come from the ambient sea water. In normal conditions, the growth of these microbes is suppressed by hemocytes and humoral factors. Otherwise, the microbes would grow rapidly and no doubt interfere with calcium carbonate precipitation, leading to shell disease. Indeed, we successfully induced shell disease in *P. fucata* by injected concentrated microbes into the EPS. The fact that the symptom was induced by microbes but not calcite particles suggests that the shell disease is ascribed to biological agents. Gram-negative bacteria and fungi are the top two important sources of disease problems in aquaculture [37]. *Vibrio tapetis* causes brown ring disease in the clam *R. philippinarum* and over-grew the infection site [29]. And the *Vibrio* bacteria also caused mass mortality of the pearl oyster *Pinctada maxima* [14]. Although the exact causes of the natural shell disease were not clear, we found that *P. fucata* was vulnerable to both bacteria and fungi infections. So, appropriate precautions would be helpful for pearl oyster aquaculture under special conditions, for example adding anti-bacterial drugs during transportation may improve oyster viability.

3.4. Hemocytes participate in the shell repair process

To further understand the shell repair process, the shells were decalcified with EDTA. A transverse section revealed that the brown deposits grew directly on the fine structure of the nacre, arranged in a longitudinal direction (Fig. 5A). This was coincident with the SEM observation that no ordered microstructures were formed at the beginning of shell repair. Strikingly, there were abundant hemocytes that formed cell layers in between the former nacre and the abnormal deposits (Fig. 5B), and these hemocyte layers disappeared at the edge of the abnormal deposits, indicating a close relation between them. Previously, granulocytes *P. fucata* were found to fuse into the regenerated prismatic layer in after shell damage [8]. The manner in which these hemocytes were buried in the shell layers was not clear. We proposed that during a serious microbial infection of the EPS, hemocytes migrate to engulf the pathogens and to promote rapid shell deposition. Indeed, large amounts of hemocytes were found in the EPS 24 h after yeast injection. These hemocytes formed clusters that agglutinated the yeast cells (Fig. 5C–E). Frequently, hemocytes containing more than one yeast cell were visible (Fig. 5F–H), indicating active phagocytosis during the infection. A great number of microbes required more time to

clean up, so some hemocytes, were buried with the invaders while the shell layers continued to precipitate.

Marine bivalves do not possess adaptive immunity, so innate immunity dominated by hemocytes is essential for resisting the infectious intruders. The ability to penetrate the tissues and reach the body surface endows hemocytes with a vast capacity to exert a cellular and humoral immune response. In Manila clams, hemocytes and enzymatic activities play crucial role in the defense process during shell disease [38]. In a similar manner to macrophages in mammals, bivalve hemocytes actively phagocytose pathogens. Therefore, hemocytes in the EPS are crucial for controlling the spread of the infectious agents. Additionally, hemocytes might contribute to shell regeneration by providing calcium and promoting $CaCO_3$ nucleation [8,39]. The supply of calcium by hemocytes during shell repair was reported in other bivalves [9,24]. Because the microstructure and texture of the shell are finely controlled, and fluctuation of the microenvironment in the EPS and variation of the expression level of the shell matrix proteins had a great impact on the shell structure [2,10,40]. The overgrowth of microbes and the influx of abundant hemocytes led to massive impurity of the EPF, thus changing the morphology of the shell and the polymorphs of the deposited $CaCO_3$. Moreover, a genetic switch in the mantle tissue might be induced by the infection, changing the secretory repertoire of the EPF subsequently changing the microstructure of the nacreous layer.

4. Conclusion

Our study showed that uncontrolled microbial growth caused a serious infection of the EPS in the pearl oyster *P. fucata*. The microstructure and polymorph of the nacreous layer were dramatically changed, but subsequently recovered during the shell repair process, and the influx of hemocytes facilitated the clearance of microbes and disrupted the normal $CaCO_3$ precipitation in the nacreous layer. We suggest that biocontrol of the microbial population is essential for the aquaculture of pearl oysters.

Authors' contributions

Jingliang Huang carried out the lab work, participated in data analysis, contributed to the design of the study and drafted the manuscript; Liping Xie and Rongqing Zhang provided financial supports and revised the manuscript. All authors gave final approval for publication.

Competing interests

The authors declare no competing financial interests.

Acknowledgements

We would like to thank Professor Xiaodong Du of Guangdong Ocean University for providing the oyster samples and Professor Junbiao Dai of Tsinghua University for providing the YFP-yeast. This work was supported by National Basic Research Program of China Grant 2010CB126405, and National Natural Science Foundation of China Grants 31372508, 31372502 and 31872543.

References

[1] H. Miyamoto, T. Miyashita, M. Okushima, S. Nakano, T. Morita, A. Matsushiro, A carbonic anhydrase from the nacreous layer in oyster pearls, Proc. Natl. Acad. Sci. U. S. A. 93 (18) (1996) 9657–9660.
[2] M. Suzuki, K. Saruwatari, T. Kogure, Y. Yamamoto, T. Nishimura, T. Kato, H. Nagasawa, An acidic matrix protein, Pif, is a key macromolecule for nacre formation, Science 325 (5946) (2009) 1388–1390.
[3] C. Liu, S. Li, J. Kong, Y. Liu, T. Wang, L. Xie, R. Zhang, In-depth proteomic analysis of shell matrix proteins of Pinctada fucata, Sci. Rep. 5 (2015) 17269.
[4] K. Nagai, A history of the cultured pearl industry, Zoolog Sci 30 (10) (2013) 783–793.
[5] T. Miyazaki, K. Goto, T. Kobayashi, T. Kageyama, M. Miyata, Mass mortalities associated with a virus disease in Japanese pearl oysters Pinctada fucata martensii, Dis. Aquat. Org. 37 (1) (1999) 1–12.
[6] C. Joubert, D. Piquemal, B. Marie, L. Manchon, F. Pierrat, I. Zanella-Cleon, N. Cochennec-Laureau, Y. Gueguen, C. Montagnani, Transcriptome and proteome analysis of Pinctada margaritifera calcifying mantle and shell: focus on biomineralization, BMC Genomics 11 (2010).
[7] M.B. Johnstone, S. Ellis, A.S. Mount, Visualization of shell matrix proteins in hemocytes and tissues of the Eastern oyster, Crassostrea virginica, J. Exp. Zool. B Mol. Dev. Evol. 310 (3) (2008) 227–239.
[8] S. Li, Y. Liu, C. Liu, J. Huang, G. Zheng, L. Xie, R. Zhang, Hemocytes participate in calcium carbonate crystal formation, transportation and shell regeneration in the pearl oyster Pinctada fucata, Fish Shellfish Immunol. 51 (2016) 263–270.
[9] N. Trinkler, J.F. Bardeau, F. Marin, M. Labonne, A. Jolivet, P. Crassous, C. Paillard, Mineral phase in shell repair of Manila clam Venerupis philippinarum affected by brown ring disease, Dis. Aquat. Org. 93 (2) (2011) 149–162.
[10] J. Xie, J. Liang, J. Sun, J. Gao, S. Zhang, Y. Liu, L. Xie, R. Zhang, Influence of the extrapallial fluid of Pinctada fucataon the crystallization of calcium carbonate and shell biomineralization, Cryst. Growth Des. 16 (2) (2016) 672–680.
[11] M.B. Johnstone, N.V. Gohad, E.P. Falwell, D.C. Hansen, K.M. Hansen, A.S. Mount, Cellular orchestrated biomineralization of crystalline composites on implant surfaces by the eastern oyster, Crassostrea virginica (Gmelin, 1791), J. Exp. Mar. Biol. Ecol. 463 (2015) 8–16.
[12] C. Paillard, P. Maes, The brown ring disease in the Manila clam, Ruditapes philippinarum: I. Ultrastructural alterations of the periostracal lamina, J. Invertebr. Pathol. 65 (2) (1995) 91–100.
[13] T. Renault, B. Chollet, N. Cochennec, A. Gerard, Shell disease in eastern oysters, Crassostrea virginica, reared in France, J. Invertebr. Pathol. 79 (1) (2002) 1–6.
[14] D.A. Pass, R. Dybdahl, M.M. Mannion, Investigations into the causes of mortality of the pearl oyster, pinctada-maxima (Jamson), in Western-Australia, Aquaculture 65 (2) (1987) 149–169.
[15] B. Allam, C. Paillard, S.E. Ford, Pathogenicity of Vibrio tapetis, the etiological agent of brown ring disease in clams, Dis. Aquat. Org. 48 (3) (2002) 221–231.
[16] R. Elston, L. Leibovitz, Pathogenesis of experimental vibriosis in larval American oysters, Crassostrea-virginica, Can. J. Fish. Aquat. Sci. 37 (6) (1980) 964–978.
[17] A.P. Maloy, S.E. Ford, R.C. Karney, K.J. Boettcher, Roseovarius crassostreae, the etiological agent of Juvenile Oyster Disease (now to be known as Roseovarius Oyster Disease) in Crassostrea virginica, Aquaculture 269 (1–4) (2007) 71–83.
[18] V. Sprague, Diseases of oysters, Annu. Rev. Microbiol. 25 (1971) 211-+.
[19] J.D. Andrews, Epizootiology of diseases of oysters (Crassostrea-virginica), and parasites of associated organisms in eastern North-America, Helgol. Meeresunters. 37 (1–4) (1984) 149–166.
[20] M.A. Ragan, G.S. MacCallum, C.A. Murphy, J.J. Cannone, R.R. Gutell, S.E. McGladdery, Protistan parasite QPX of hard-shell clam Mercenaria mercenaria is a member of Labyrinthulomycota, Dis. Aquat. Org. 42 (3) (2000) 185–190.
[21] M. Almeida, F. Berthe, A. Thebault, M.T. Dinis, Whole clam culture as a quantitative diagnostic procedure of Perkinsus atlanticus (Apicomplexa, Perkinsea) in clams Ruditapes decussatus, Aquaculture 177 (1–4) (1999) 325–332.
[22] C. Zhang, R.Q. Zhang, Matrix proteins in the outer shells of molluscs, Mar. Biotechnol. 8 (6) (2006) 572–586.
[23] Y. Yan, D. Yang, X. Yang, C. Liu, J. Xie, G. Zheng, L. Xie, R. Zhang, A novel matrix protein, PfY2, functions as a crucial macromolecule during shell formation, Sci. Rep. 7 (1) (2017) 6021.
[24] A.S. Mount, A.P. Wheeler, R.P. Paradkar, D. Snider, Hemocyte-mediated shell mineralization in the eastern oyster, Science 304 (5668) (2004) 297–300.
[25] L. Xiang, W. Kong, J.T. Su, J. Liang, G.Y. Zhang, L.P. Xie, R.Q. Zhang, Amorphous calcium carbonate precipitation by cellular biomineralization in mantle cell cultures of Pinctada fucata, PLoS One 9 (11) (2014).
[26] L.S. Gomez-Villalba, P. Lopez-Arce, R. Fort, Nucleation of CaCO3 polymorphs from a colloidal alcoholic solution of Ca(OH)(2) nanocrystals exposed to low humidity conditions, Appl Phys a-Mater 106 (1) (2012) 213–217.
[27] C. Fleury, F. Marin, B. Marie, G. Luquet, J. Thomas, C. Josse, A. Serpentini, J.M. Lebel, Shell repair process in the green ormer Haliotis tuberculata: a histological and microstructural study, Tissue Cell 40 (3) (2008) 207–218.
[28] E. Kadar, A. Lobo-da-Cunha, C. Azevedo, Mantle-to-shell CaCO3 transfer during shell repair at different hydrostatic pressures in the deep-sea vent mussel Bathymodiolus azoricus (Bivalvia: Mytilidae), Mar. Biol. 156 (5) (2009) 959–967.
[29] C. Paillard, P. Maes, The brown ring disease in the Manila clam, Ruditapes philippinarum: II. Microscopic study of the brown ring syndrome, J. Invertebr. Pathol. 65 (2) (1995) 101–110.
[30] V.R. Meenakshi, P.L. Blackwelder, P.E. Hare, K.M. Wilbur, N. Watabe, Studies on shell regeneration. I. Matrix and mineral composition of the normal and regenerated shell of Pomacea paludosa, Comp. Biochem. Physiol. A Comp. Physiol. 50 (2) (1975) 347–351.
[31] P. Bots, L.G. Benning, R.E.M. Rickaby, S. Shaw, The role of SO4 in the switch from calcite to aragonite seas, Geology 39 (4) (2011) 331–334.
[32] B. Marie, C. Joubert, A. Tayale, I. Zanella-Cleon, C. Belliard, D. Piquemal, N. Cochennec-Laureau, F. Marin, Y. Gueguen, C. Montagnani, Different secretory repertoires control the biomineralization processes of prism and nacre deposition of the pearl oyster shell, Proc. Natl. Acad. Sci. U. S. A. 109 (51) (2012) 20986–20991.
[33] M. Fritz, A.M. Belcher, M. Radmacher, D.A. Walters, P.K. Hansma, G.D. Stucky, D.E. Morse, S. Mann, Flat pearls from biofabrication of organized composites on inorganic substrates, Nature 371 (6492) (1994) 49–51.
[34] L. Xiang, J.T. Su, G.L. Zheng, J. Liang, G.Y. Zhang, H.Z. Wang, L.P. Xie, R.Q. Zhang, Patterns of expression in the matrix proteins responsible for nucleation and growth of aragonite crystals in flat pearls of Pinctada fucata, PLoS One 8 (6) (2013).

[35] S. Li, Y. Liu, C. Liu, J. Huang, G. Zheng, L. Xie, R. Zhang, Morphology and classification of hemocytes in Pinctada fucata and their responses to ocean acidification and warming, Fish Shellfish Immunol. 45 (1) (2015) 194–202.
[36] J.L. Huang, S.G. Li, Y.J. Liu, C. Liu, L.P. Xie, R.Q. Zhang, Hemocytes in the extrapallial space of Pinctada fucata are involved in immunity and biomineralization, Sci Rep-Uk 8 (2018).
[37] F.P. Meyer, Aquaculture disease and health management, J. Anim. Sci. 69 (10) (1991) 4201–4208.
[38] B. Allam, K.A. Ashton-Alcox, S.E. Ford, Haemocyte parameters associated with resistance to brown ring disease in Ruditapes spp. clams, Dev. Comp. Immunol. 25 (5–6) (2001) 365–375.
[39] E. Kadar, Haemocyte response associated with induction of shell regeneration in the deep-sea vent mussel Bathymodiolus azoricus (Bivalvia : Mytilidae), J. Exp. Mar. Biol. Ecol. 362 (2) (2008) 71–78.
[40] J. Liu, D. Yang, S.T. Liu, S.G. Li, G.R. Xu, G.L. Zheng, L.P. Xie, R.Q. Zhang, Microarray: a global analysis of biomineralization-related gene expression profiles during larval development in the pearl oyster, Pinctada fucata, BMC Genomics 16 (2015).